

A Knowledge Distillation Framework for Predicting Short and Long-term Hospitalisation Outcomes from Electronic Health Records Data

Zina M Ibrahim, Daniel Bean, Thomas Searle, Honghan Wu, Anthony Shek, Zeljko Kraljevic, James Galloway, Sam Norton, James T Teo, Richard JB Dobson

Abstract—The ability to perform accurate prognosis of patients is crucial for proactive clinical decision making, informed resource management and personalised care. Existing outcome prediction models suffer from a low recall of infrequent positive outcomes. We present a highly-scalable and robust machine learning framework to automatically predict adversity represented by mortality and ICU admission from time-series vital signs and laboratory results obtained within the first 24 hours of hospital admission. The stacked platform comprises two components: a) an unsupervised LSTM Autoencoder that learns an optimal representation of the time-series, using it to differentiate the less frequent patterns which conclude with an adverse event from the majority patterns that do not, and b) a gradient

boosting model, which relies on the constructed representation to refine prediction, incorporating static features of demographics, admission details and clinical summaries. The model is used to assess a patient's risk of adversity over time and provides visual justifications of its prediction based on the patient's static features and dynamic signals. Results of three case studies for predicting mortality and ICU admission show that the model outperforms all existing outcome prediction models, achieving PR-AUC of 0.93 (95% CI: 0.878 - 0.969) in predicting mortality in ICU and general ward settings and 0.987 (95% CI: 0.985-0.995) in predicting ICU admission.

Index Terms—Ensemble Learning, Gradient Boost, Imbalanced time-series, Long Short Term Memory networks (LSTM), Medical Outcome Prediction, Outlier Detection, Machine Learning, Mortality Prediction, Stacked Ensemble Learning, Time-series Forecasting.

I. INTRODUCTION

The task of predicting hospitalisation outcomes from multivariate time-series is well-studied in the literature. Existing models range from ad-hoc early warning scoring systems based on aggregates of manually-selected physiological measurements [34] and machine learning models [8]. A prominent example of early warning scores is the National Early Warning Score (NEWS2) [44], which has received formal endorsement by the United Kingdom's National Health Services to become the early warning system for identifying acutely ill patient. NEWS2 is representative of early warning scores in assuming independence among the predictive variables measured [22], subsequently failing to capture the dependencies among the temporal signatures of the patient's physiology. In contrast, machine learning models overcome this limiting factor using sophisticated architectures to capture the non-linearities within the multivariate temporal data [8]. However, we find that existing machine learning approaches suffer from several problems. First, most of the current models have either been tested on a single condition (e.g. sepsis [23], cardiac patients [26], COVID-19 [57], brain injury [43]), or solely target Intensive Care Unit (ICU) settings [3], [53], where the magnitude of measurements is high, and the population is more uniform in the level of acuity (the interested reader can refer to [48] for a comprehensive review). Second, none of the existing models has been evaluated using metrics that accurately describe

Submitted on 16/11/2020. DMB is funded by a UKRI Innovation Fellowship as part of Health Data Research UK MR/S00310X/1. ZI and RJBD are supported by (1) NIHR Biomedical Research Centre at South London and Maudsley NHS Foundation Trust and King's College London, London, U.K. (2) National Institute for Health Research (NIHR) Biomedical Research Centre at South London and Maudsley NHS Foundation Trust and King's College London, and (3) the National Institute for Health Research University College London Hospitals Biomedical Research Centre. RJBD is further supported by (1) Health Data Research UK, which is funded by the UK Medical Research Council, Engineering and Physical Sciences Research Council, Economic and Social Research Council, Department of Health and Social Care, Chief Scientist Office of the Scottish Government Health and Social Care Directorates, Health and Social Care Research and Development Division, Public Health Agency, British Heart Foundation and Wellcome Trust (2) The BigData@Heart Consortium, funded by the Innovative Medicines Initiative-2 Joint Undertaking under grant agreement No. 116074. AS is supported by a King's Medical Research Trust studentship. HW is supported by Medical Research Council and Health Data Research UK Grant (MR/S004149/1) and Wellcome Institutional Translation Partnership Award (P111054). JTHT is supported by London AI Medical Imaging Centre for Value-Based Healthcare (AI4VBH) and the National Institute for Health Research (NIHR) Applied Research Collaboration South London (NIHR ARC South London) at King's College Hospital NHS Foundation Trust.

ZM Ibrahim, D Bean, T Searle, Z Kraljevic and RJB Dobson are with the Department of Biostatistics and Health Informatics, King's College London, SE5 8AF UK ({zina.ibrahim; daniel.bean; thomas.searle; zeljko.kraljevic; richard.j.dobson}@kcl.ac.uk).

H Wu and RJB Dobson are with the Institute of Health Informatics, University College London, UK ({honghan.wu; r.dobson}@ucl.ac.uk).

A Shek is with the Department of Clinical Neuroscience, King's College London, London, UK (anthony.shek@kcl.ac.uk)

J Galloway is with the Centre for Rheumatic Diseases, King's College London (james.galloway@kcl.ac.uk)

S Norton is jointly appointed by the Department of Psychology and the Department of Inflammation Biology, King's College London (sam.norton@kcl.ac.uk)

J Teo is with King's College Hospital NHS Foundation Trust (james-teo@nhs.net).

the model's ability to predict (the less frequent) outcomes (e.g. mortality). To clarify, consider the United Kingdom's in-hospital mortality rates, which are around 23% in ICU settings [2] and 4% in secondary hospital wards [17]. If one thinks of outcome prediction as a binary classification problem, then it is undoubtedly one with a highly skewed distribution of the target variable (mortality in this case); with samples corresponding to survival being orders of magnitude larger than those corresponding to a positive outcome. In such a problem, the classifier's predictions should align with the user preference bias towards performance on poorly represented cases [5]. Despite this, the majority of the general outcome prediction models, i.e. those that are not constrained by a condition or patient population type [1], [7], [33], [49], generally rely on achieving a high Receiver-Operator Curve Area Under the Curve (ROC-AUC) without considering the metric's impartial assessment towards the imbalanced outcomes [13]. Finally, in contrast to medical practice, where the combined view of physiological sign changes and patient characteristics (e.g. demographics, pre-existing conditions) used to make a prognosis, the combination of multivariate temporal signatures and variables underlying patient characteristics has either been examined descriptively and not in the context of a predictive model [4], or distinctly without consideration of the interplay between the two [47]. There is, therefore, a missed opportunity in developing forecasting models that combine dynamic time-series with static features as done in other domains, e.g. [32].

To overcome the above difficulties, we propose the reformulation of the task of outcome prediction from multivariate time series hospital data into one of *outlier detection*, whereby positive outcomes (e.g. mortality =1) are regarded as outliers. We subsequently develop a 2-level stacked machine learning architecture centred around an unsupervised LSTM-AutoEncoder module trained on the majority (negative outcome) samples, using it to learn a compressed representation of the temporal context that distinguishes those from 'outliers'. The learned context captures the multivariate interactions in the time-series. It is also used to guide a gradient boost module to estimate the risk of adversity using static data comprising summary statistics of vital signs and laboratory tests, demographics and admission details. The two modules, therefore, jointly make predictions using a combined view of a patient's state, based on the temporal signatures and static data. The stacked architecture is equipped with a justification module to generate visual justifications of the predicted outcomes.

II. RELATIONSHIP TO EXISTING FRAMEWORKS

LSTM AutoEncoders have shown competitive accuracy in detecting outliers from multivariate time-series data [28], [29]. They do so by encoding the time-series in a low dimension to capture its most representative features. Since the encoded representation is compact, it is only possible to reconstruct representative features from the input, not the specifics of the input data, including any outliers [28]. These models have been effectively used in fall detection [40], sensor failure prediction [36], fraud detection [15] and video surveillance [55]. Despite their potential as solutions for healthcare problems, their

use has been limited to retinal eye research [45] and fraud detection in healthcare settings [51].

The problem of outcome prediction from hospitalisation data has recently witnessed the design of numerous ensemble architectures to enhance model performance and to support interpretability. Ensemble models have shown superior performance as compared to single-classifier architectures, either by enhancing predictive capability by different data modalities (i.e. a static view and a dynamic view) [47], or by consolidating predictions of several 'weak' predictors in an additive way (e.g. voting) [54]. However, model combination in an ensemble is often performed during the prediction stage, which is problematic regardless of the type of ensemble used. In ensembles operating on different data modalities, the final prediction is not representative of the possible dependencies between the static view (e.g. demography, pre-existing conditions, etc.) and the dynamic view (the temporal interactions embedded within the time-series) [32]. Similarly, ensembles of several weak classifiers have been shown to fail in alleviating the bias of the individual learners, and are generally outperformed by alternative models that *stack* strong classifiers into an ensemble [10]. These two observations are related to how existing models are evaluated in the literature. Specifically, all existing ensemble models unanimously use the Receiver-Operator Curve (ROC) space for evaluation [7], [30], [35], [42], [49]. However, the ROC space is known to be highly optimistic of classification performance when using highly-skewed datasets and where the interest lies in the correct prediction of the minority class [9]. Such conditions are representative of the problem of predicting (the less likely) adverse outcomes from Electronic Health Records (EHR) data.

III. CONTRIBUTIONS

The contribution of this work is the design and validation of an end-to-end machine learning framework to predict hospitalisation outcomes over increasing intervals. The framework possesses several attractive features that complement the literature in the following ways:

- 1) The framework is robust to the marginal representation of positive outcomes in a given population; this is achieved by regarding hospitalisation outcomes as outliers and making use of a successful outlier detection architecture as the base for prediction.
- 2) The framework captures the true interplay between the temporal signatures of a patient's physiology and static clinical summaries commonly used by practitioners in clinical settings. This is achieved via a stacked ensemble architecture whereby a compressed representation of the temporal signatures drives a classification model based on static features.
- 3) The framework is capable of justifying its predictions through visual illustrations. The justifications highlight the most contributing temporal signatures of the patient's physiology, as well as the static features, to the predicted outcome.
- 4) Evaluating the framework using PR-AUC and macro-averaged precision, recall and F1-score on real patient

time-series data shows robustness over the diversity of patient populations (ICU data and secondary hospital wards; pneumonia, chronic kidney disease (CKD) and COVID-19 outcomes), outcome distributions, sample size, and short and long-term outcomes.

IV. TERMINOLOGY AND MODEL FORMULATION

In this work, vectors are represented by boldface lower-case letters and matrices by boldface upper case letters. Unless specified, all vectors are assumed to be row vectors. The multivariate time-series input data $D^d = \{X_p^d\}_{p=1}^n$ for n patients is observed as:

$$X_1^d, X_2^d, \dots, X_n^d$$

Where X_p^d contains the totality of the dynamic observations for patient p in the sample. Furthermore:

$$X_p^d = \begin{bmatrix} x_{p1}^d \\ \vdots \\ x_{pT}^d \end{bmatrix}$$

Where T is the number of observations per patient and each vector $x_p \in \mathbb{R}^v$ denotes the feature space consisting of a sequence of v vital signs or laboratory results dynamically accrued during the first 24 hours of admission. Furthermore, the static input data is $D^s = \{x_p^s\}_{p=1}^n$ where $x_p^s \in \mathbb{R}^u$ denotes the feature space consisting of a sequence of u static variables which may correspond to demography, pre-existing conditions or summary statistics of clinical variables. Finally, $y_o^i = \{y_p\}_{p=1}^n$ is a column vector corresponding to the true incidence of outcome o during interval i for each patient p .

The goal of the framework is to predict:

$$\hat{p}_o^i, \hat{y}_o^i = \begin{bmatrix} \hat{p}_{o1}^i, \hat{y}_{o1}^i \\ \vdots \\ \hat{p}_{on}^i, \hat{y}_{on}^i \end{bmatrix}$$

Each $\hat{y}_o^i \in [0, 1]$ is a binary variable representing the predicted onset of adverse outcome o during interval i for a single patient; \hat{p}_o^i is the predicted probability of the outcome \hat{y}_o^i , which we retain for use during the interpretation stage. In this paper $o \in \{\text{Mortality}, \text{ICU Admission}, \text{ICU ReAdmission}\}$ and $i \in \{5\text{Day}, 7\text{Day}, 14\text{Day}, 30\text{Day}\}$. Naturally, the class distribution of \hat{y}_o^i is highly imbalanced in favour of the negative outcome, as will be demonstrated in the evaluation sections.

In the framework presented here, the probability of outcome o during interval i , \hat{p}_o^i , is learned using the two views of the clinical data D^d and D^s and is used to estimate \hat{y}_o^i .

V. THE ARCHITECTURE

As the resulting time-series classification problem is one with imbalanced samples, the framework is designed to capitalise on the lower frequency of positive outcomes (e.g. ITU admission = 1) with respect to negative outcomes (e.g. no ITU admission) in the overall population. This is done by

first ‘self-training’ using a subset of the negative samples of D^d in order to learn a compressed representation describing the multivariate temporal dependencies within the majority (no adversity) population, enabling the evaluation of any incoming time-series for deviation from the majority (i.e. positive outcomes). The learned representation is then used to complement outcome prediction from the static view of the data D^s .

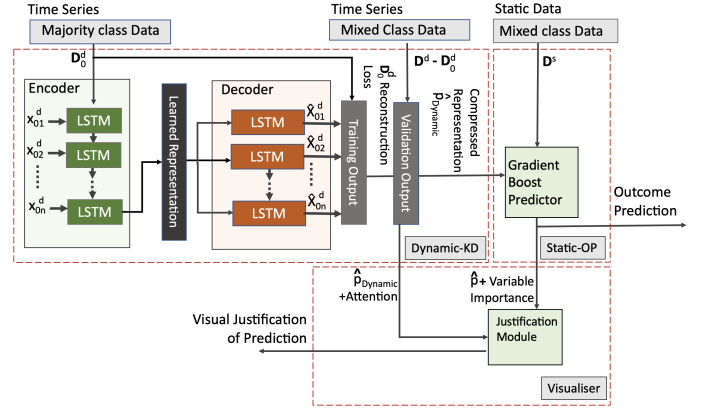


Fig. 1: KD-OP Pipeline

The overall framework is shown in Figure 1 and comprises two modules stacked to predict \hat{p}_o^i and \hat{y}_o^i . Each of the two modules is designed to learn a view of the data: *Dynamic-KD* (KD: Knowledge Distiller) learns a uni-dimensional representation $\hat{p}_{oDynamic}^i \in [0 - 1]$ from the time-series such that for two individuals a and b whose time-series observations X_a^d and $X_b^d \in D^d$, if $\hat{y}_{o_a}^i > \hat{y}_{o_b}^i$ then :

$$[\log(\hat{p}_{o_aDynamic}^i)] > [\log(\hat{p}_{o_bDynamic}^i)]$$

That is, the vector representation $\hat{p}_{oDynamic}^i$ creates a separation between negative and positive-outcome time-series. The joint use of log transformation and flooring captures the difference in the order of magnitude of the resulting representations, rather than possibly non-significant fluctuations within the actual values [11].

The second module, *Static-OP* (OP: Outcome Predictor) combines $\hat{p}_{oDynamic}^i$ with D^s to estimate the final prediction probability \hat{p}_o^i . Static-OP is a classification ensemble based on gradient boost trees. The two modules form a bi-level stacked classification system we call *KD-OP* (Knowledge-Distillation Outcome Predictor). The output for the ensemble is:

$$\hat{y}_o^i = \begin{cases} 0 & \text{if } \hat{p}_{oStatic}^i > \gamma \\ 1 & \text{otherwise} \end{cases} \quad (1)$$

Where $\gamma \in [0 - 1]$ is a learned parameter corresponding to the optimal threshold for classification selected by optimising the mean Area Under the Precision-Recall Curve (PR-AUC) in the validation set.

KD-OP provides a visual justification of its predicted \hat{y}_o^i for a given outcome o during interval i . The justification component combines the attention vector generated by *Dynamic-KD* and the relative importance of the static features generated

by *Static-OP* along with the relative contribution of the two modules to the final prediction. The remainder of this section details the design of *KD-OP*'s individual modules.

A. Dynamic-KD

The multivariate time-series are first processed by *Dynamic-KD*, which consists of an unsupervised LSTM-Autoencoder architecture trained to reconstruct the input sequence by minimizing a distance-based objective function \mathcal{J} . \mathcal{J} measures the difference between the input vectors in the original series \mathbf{X}_p^d and the vectors of the reconstructed series $\hat{\mathbf{X}}_p^d$ for each batch (patient) p in \mathbf{D}^d . \mathcal{J} is defined as below:

$$\mathcal{J} = \sqrt{\sum_{i=1}^m \|\mathbf{x}_i - \hat{\mathbf{x}}_i\|_2^2} \quad (2)$$

Where m is the number of multivariate observations for each patient p and $\|\cdot\|_2$ is the L2-norm of a given vector.

Dynamic-KD adopts an attention mechanism over the time steps to capture the most important features in each sequence as proposed by [19] and successfully implemented in [46], [49], [50]. Figure 2 shows a feature-level representation of the attention mechanism in the encoder-decoder architecture of *Dynamic-KD*, reconstructing a multi-variable sequences over T time step batches (i.e. T ordered sequences per patient). For each feature j , a soft attention mechanism is implemented over the encoder's hidden states to obtain a distinct context vector \mathbf{c}_j . \mathbf{c}_j attenuates the most informative hidden states in $s_{j,1}, \dots, s_{j,T}$ of the decoder and is computed as follows:

For each feature j , the attention probabilities based on the encoded sequence $\alpha = (\alpha_1, \dots, \alpha_T)$ are calculated using the encoded sequence and the encoder's internal hidden states. First, the importance of information at each time step for feature j is calculated:

$$e_{j,t} = a(\mathcal{U}_j \otimes s_{t-1} + \mathcal{W}_j \otimes h_j + b_j)$$

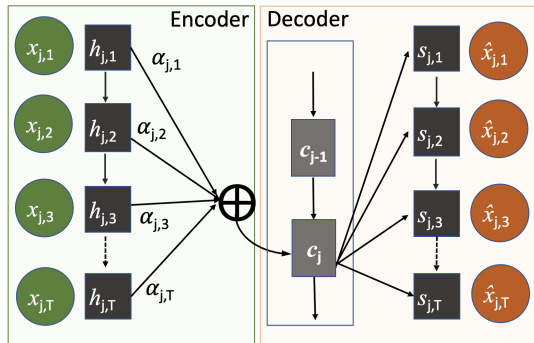


Fig. 2: The attention mechanism of the encoder-Decoder Architecture demonstrated at feature level.

Where \mathcal{U}_j and \mathcal{W}_j are trainable parameters capturing the input-to-hidden and hidden-to-hidden transitions for a given layer j respectively. Terms $\mathcal{W}_j \otimes h_{t-1}$ and $\mathcal{U}_j \otimes x_t$ respectively capture the update from the hidden states at the previous step and the new input. a is the activation function.

In the decoder layers, we can measure the importance of the information at each time step for each feature j denoted by $e_{j,t}$ using proximity to \mathcal{U}_j . Then $\alpha_{j,t}$ is obtained by normalising $e_{j,t}$ using the softmax operation:

$$\alpha_{j,t} = \frac{\exp(e_{j,t})}{\sum_{t=1}^T \exp(e_{j,t})}$$

Finally, the context vector for each feature \mathbf{c}_j is calculated using the weighted sum of the encoded sequence with the attention probabilities. Intuitively, this vector summarizes the importance of the encoded features in predicting t^{th} sequence:

$$\mathbf{c}_j = \sum_{t=1}^T \alpha_{j,t} h_{j,t} \quad (3)$$

The *Dynamic-KD* LSTM-Autoencoder is trained in batches as shown in Algorithm 1. Training is done strictly on the negative-outcome data (the majority class), which we term $\mathbf{D}_{Train,0}^d$ (line 1), to minimise the reconstruction loss \mathcal{J} (line 2). The resulting loss is therefore representative of the training errors associated with the negative (majority) class.

Algorithm 1: Dynamic-KD

Receives: Training and validation subsets of the multivariate, regularly-sampled and batched time-series, $\mathbf{D}_{Train}^d = \{\mathbf{X}_p^d\}_{p=1}^{z_1}$ for z_1 patients in the training set and $\mathbf{D}_{Valid}^d = \{\mathbf{X}_p^d\}_{p=1}^{z_2}$ for z_2 patients in the validation set.

Returns: Validation reconstruction loss $\hat{p}_{Dynamic}$, and attention matrix \mathbf{C}_{Valid}

Train Auto Encoder

- 1 Extract $\mathbf{D}_{Train,0}^d$ from \mathbf{D}_{Train}^d
- 2 $\hat{\theta} = \underset{\theta}{\operatorname{argmin}} \mathcal{J}(\mathbf{X}_{Train,0}^d)$

Validate Auto Encoder

- 3 $\hat{\mathbf{D}}_{Valid}^d, \mathbf{C}_{Valid} = \text{Decoder}(\text{Encoder}(\mathbf{X}_{Valid}^d), \hat{\theta})$
 - 4 $\hat{p}_{Dynamic} = \hat{\mathbf{D}}_{Valid}^d - \mathbf{D}_{Valid}^d$
-

The LSTM-Autoencoder is validated using a non-overlapping subset of the time-series \mathbf{D}_{Valid}^d (line 3), which contains mixed data (positive and negative outcomes), using the optimal loss obtained during training. Validation yields a reconstruction $\hat{\mathbf{D}}_{Valid}^d$ of \mathbf{D}_{Valid}^d and an attention matrix \mathbf{C}_{Valid} . At the end of the procedure, the difference between the original and reconstructed validation sets augments the original highly-dimensional feature space into a linear representation which is descriptive of the deviation from normality (no adversity) with respect to the temporal interactions embedded within the data. The validation reconstruction loss $\hat{p}_{Dynamic}$ (line 4) is therefore discriminatory between the two classes and corresponds to the likelihoods of each batch (patient) p , where $1 \leq p \leq z_2$, belonging to the positive class. $\hat{p}_{Dynamic}$ is used to complement the learning from static

features performed by *Static-OP*, while C_{Valid} is fed into the explainer component of the framework.

B. Static-OP

The goal of this module is to complement the predictions made through the temporal representation learned by *Dynamic-KD* using static information routinely employed by healthcare practitioners to assess a patient's risk factors (e.g. demographics, symptoms, summary statistics of physiology). In other words, instead of using $\hat{p}_{Dynamic}$ as a predictor of the outcome, it is instead used to drive further classification using static features via a gradient boosting model [27]. This way, the overall pipeline has the advantage of capturing the interplay between dynamic physiological measurements and static features in making the final predictions. The overall structure of *Static-OP* is given in Algorithm 2. First, *Static-OP* is trained using D_{Valid}^s and y_{Valid} , with the reconstruction errors $\hat{p}_{Dynamic}$ serving as sample weights ω (line 1). Because *Dynamic-KD* ensures that $\hat{p}_{Dynamic}$ creates a separation between positive and negative classes, the minority samples of D_{Valid}^s will be the determinant of the decision threshold the model is trained to discover. Using the model to predict the outcome probabilities from y_{Test} produces the predicted probabilities \hat{p} , and will also produce the variable importance vector (line 2). The class labels \hat{y} , are obtained as in Equation 1 (line 4), using a prediction threshold learned by maximising the precision-recall area under the curve from the predicted probabilities (line 3).

Algorithm 2: Static-OP

Receives:

- 1) Validation and testing subsets of the original dataset containing static features $D_{Valid}^s = \{X_p^s\}_{p=1}^{z_2}$ for z_2 patients in the validation set and $D_{Test}^s = \{X_p^s\}_{p=1}^{z_3}$ for z_3 patients in the test set.
- 2) True validation and testing class labels y_{Valid} and y_{Test}
- 3) Validation reconstruction loss, $\hat{p}_{Dynamic}$ for z_2 patients in the validation set, obtained from *Dynamic-KD*.

Returns : Classification label \hat{y} , $\hat{y} \in [0, 1], \forall \hat{y} \in \hat{y}$, variable importance \mathcal{I}

Train Gradient Boost

- 1 $\mu =$
TrainGB($X = D_{Valid}^s, y = y_{Valid}, \omega = \hat{p}_{Dynamic}$)
 - Test Gradient Boost**
 - 2 $\hat{p}, \mathcal{I} = \mu(D_{Test}^s, y_{Test})$
 - 3 $\gamma = \underset{PR-AUC}{\operatorname{argmax}} (y_{test}, \hat{p}_{test})$
 - 4 $\hat{y} \geq \hat{p}^\gamma$
-

VI. EXPERIMENTAL EVALUATION ON REAL USE CASES

We critically assess the model's performance in predicting mortality, as well as unplanned ICU admission and readmission via three different case studies: COVID-19 outcomes

using general ward hospital data, and pneumonia and chronic kidney disease (CKD) outcomes using ICU data. The three use cases were chosen to represent different demographical and outcome distributions, as will be detailed in Section VI-A. The model is used to predict mortality in all studies but is only used to predict ICU admission in the COVID-19 dataset. Instead, since pneumonia and CKD use-cases are based on ICU time-series, the model is used to predict ICU readmission. The risks of all adverse outcomes are predicted at intervals of 5, 7, 14 and 30 days within hospital admission.

A. Datasets

1) *COVID-19 Case Study* : Data was collected from 1,276 adults (≥ 18 years old) inpatients of two acute hospitals: King's College Hospital and Princess Royal University Hospital in South East London, UK. All patients in the dataset tested positive for SARS-CoV2 between the 1st of March and 31st April 2020. Static data collected include age, gender, ethnic background, the length of the period from symptoms onset to hospital admission, and pre-existing conditions (specifically, chronic obstructive pulmonary disease (COPD), Asthma, heart failure, diabetes, ischemic heart disease (IHD), hypertension and chronic kidney disease). For training and risk prediction, pre-existing conditions were aggregated into one ordinal feature describing the number of comorbidities at the time of admission. The dynamic features included 14 routinely collected vital signs and laboratory tests and are available on our online repository¹.

2) *Pneumonia and CKD Case Studies*: We used the data of ICU stays between 2001 and 2012 obtained from the anonymized Medical Information Mart for Intensive Care III (MIMIC-III) database, which is a freely-available anonymised ICU database and is the largest resource of time-series hospital data available worldwide [25]. We extracted admission details, demographics, time-stamped vital signs and laboratory test results obtained over the first 24 hours of admission of ICU stays of adults having ICD-9 code = 482.9 (pneumonia, cause not otherwise specified) and 585.9 (CKD, cause not otherwise specified) recorded as the primary diagnoses in the ICU admission notes. Since the MIMIC-III database is structured such as each hospital admission may correspond to multiple ICU stays, we extract the time-series pertaining to the first ICU stay of each admission, and used subsequent ICU admission to describe readmission outcomes. The resulting datasets comprise 509,323 records corresponding to 2,798 pneumonia ICU stays and 702,813 records corresponding to 2,822 CKD ICU stays (SQL and python scripts for recreating the dataset using the MIMICIII database are available on our online repository²).

3) *Data Description and Characteristics*: Table I provides statistical summaries of the three datasets. The datasets vary in size, where pneumonia and CKD are much larger than COVID-19. The difference in size is a direct consequence of the mode of collection. The pneumonia and CKD datasets

¹<https://github.com/zibrahim/MIMICTimeSeriesProcessing/blob/main/VitalAggregation.pdf>

²<https://github.com/zibrahim/MIMICTimeSeriesProcessing>

were extracted from the largest publicly-available ICU time-series database [25], while the COVID-19 data was locally collected over a short time span. Females were only the majority of cases in the COVID-19 dataset (females = 57.6 %), but gender distribution only significantly differed from the CKD dataset (females = 37.27%) and not from the pneumonia dataset (females = 45.58%). The pneumonia cohort was significantly younger and less co-morbid than the other two. The pneumonia cohort also showed a wider distribution of age compared to COVID-19 and CKD. In addition, the table shows that the number of pre-existing conditions varied greatly in the pneumonia and CKD cohorts, while the distribution of pre-existing conditions was more uniform in the COVID-19 dataset. The different distributions in age and pre-existing conditions is quite reasonable and align with the nature of the use cases: CKD is an age-related chronic illness [37], with previous studies showing that the rate of comorbidities is around 41% [31]. COVID-19 hospital admissions are more likely in the elderly with pre-existing conditions such as hypertension and diabetes, where symptoms are likely to be more severe as opposed to the young healthy individuals [41]. In contrast, although both older age and pre-existing conditions increase the risk of acquiring pneumonia, they have not been found to be associated with the severity of the condition and subsequent intensive care needs [39], [52].

Across all prediction intervals, the COVID-19 dataset had higher rates of mortality, while mortality rates of CKD were significantly lower than the other two cohorts. In addition, the CKD cohort had significantly lower rates of ICU admissions across all prediction intervals compared to the other two cohorts. However, the time to ICU admission was much lower in COVID-19, where the average duration from admission to ICU admission was 4.35 days, compared to 12.23 days in pneumonia and 11.18 days in CKD.

Attribute	COVID-19 (General Ward)	Pneumonia ICU	CKD (ICU)
Patients, n	1,276	2,798	2,822
Females	735(57.6 %)	1,217(45.58%)	1,139 (37.27%)
Age	69.3 (16.79)	50.05 (33.93)	72.61 (22.55)
No. Comorbidities	0.32 (0.14)	0.22 (0.18)	0.29 (0.19)
Mortality			
5-Day	139 (10.88%)	183 (6.48%)	169 (5.98%)
7-Day	187(14.64%)	257 (9.19%)	222 (7.87%)
14-Day	264 (20.68)	412 (14.73%)	310 (10.98%)
30-Day	335 (26.23%)	530 (18.94%)	378 (13.39%)
Days to mortality	12.07 (15.59)	15.38 (12.46)	11.87 (14.44)
ICU	12.07 (15.59)	15.38 (12.46)	11.87 (14.44)
5-Day	105 (8.22 %)	63 (2.36%)	78 (2.81%)
7-Day	112 (8.77%)	102 (3.82%)	80 (2.84%)
14-Day	123 (9.63%)	199 (7.45%)	157 (5.56%)
30-Day	124 (9.71%)	272 (10.18%)	196 (6.95%)
Days to ICU	4.35(8.30)	12.23 (10.46)	11.18 (10.49)

TABLE 1: Summary statistics of the datasets. Data are displayed as mean (standard deviation) or count (percent). The number of pre-existing conditions were scaled to [0-1] as the two data sources used different scales to measure co-morbidity. ICU refers to ICU admission in the COVID-19 study and ICU re-admission in MIMIC-III.

B. Data Preprocessing

The three data extracts comprised irregularly-sampled time sequences of the vital signs. Using the extracted data to train *KD-OP* required transforming the irregular time series into $D^d = \{X_1^d, \dots, X_n^d\}$ for the n patients, where each X_p^d is a $T \times v$ matrix, T is a fixed number of observations and v is the number of vital signs measured at each time window $t \in T$. To alleviate missingness and to overcome non-uniform sampling, we deployed a patient-specific interval-based aggregation of the multivariate time-series whereby the length of the aggregation window was chosen via an iterative process aiming to maximise completeness while minimising the length of the aggregation window. For each aggregation window, if a vital sign has multiple observation, then those are aggregated using a knowledge-based approach that mimics the summaries used by clinicians for each variable in practical settings and are available on our online repository³. The procedure produced $T = 48$ for pneumonia and CKD (aggregation into half-hourly intervals) and $T = 12$ for the COVID-19 use-case (aggregation into 2-hourly intervals). The resulting datasets comprised 30,624 samples with 12 variables for the COVID-19 dataset, 134,304 and 135,456 samples with 30 variables for the pneumonia and CKD cases respectively. The datasets were further imputed using a batch-aware Gaussian Process Regression model to interpolate the posterior mean and variance for the missing observations for each feature.

The datasets have two distinguishing properties: 1) the outcomes are skewed, with positive outcomes being highly under-represented in the time-series, and 2) the temporal ordering is defined over T batches, where each batch corresponds to a single patient. In order to retain the natural distribution of outcomes and temporal ordering during training and validation and to prevent information leakage, we used stratified grouped k-fold cross validation⁴, with $k=3$, to split the data for training, validation and testing sets as shown in Figure 3. At each iteration, the data used to train *Dynamic-KD* was obtained using one fold, discarding the samples corresponding to patients with positive outcomes to yield $D_{Train,0}^d$. The second fold was used as a validation set of *Dynamic-KD*, in order to obtain $\hat{y}_{DynamicVal}$ for the validation set and further to train *Static-OP*, using $\hat{y}_{DynamicVal}$ as sample weights. The third fold was first used to predict the testing $\hat{y}_{DynamicTest}$ using *Dynamic-KD* and to test the performance of *Static-OP*, using the testing $\hat{y}_{DynamicTest}$ as sample weights.

Furthermore, the data was normalised prior to training using a number of scaling techniques including absolute-value scaling, standard scaling and min-max scaling. Using a min-max scaler with a range of $[0 - 1]$ achieved the best classification performance and was therefore adopted for all the models. It should be noted that the data was scaled at each split as opposed to prior to splitting the data in order to ensure that the testing data is completely novel to the models. At each split, the training data was used to fit the scaler to

³<https://github.com/zibrahim/MIMICTimeSeriesProcessing/blob/main/VitalAggregation.pdf>

⁴<https://www.kaggle.com/jakubwasikowski/stratified-group-k-fold-cross-validation>

obtain the shift and scale statistics used to further normalise the validation and testing data.

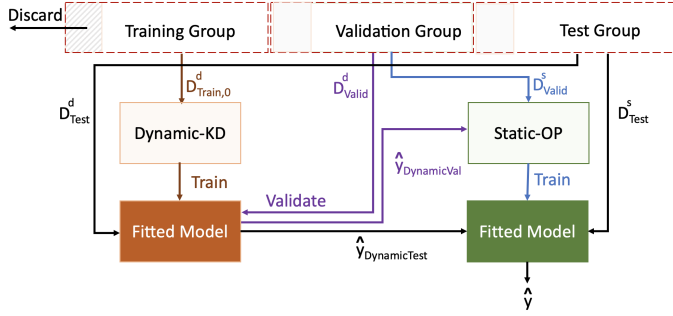


Fig. 3: The procedure followed for splitting the datasets into training, validation and testing sets used by *KD-OP*.

C. Model Selection

We used the Python language and the Keras library with Tensorflow backend⁵. For *Dynamic-KD*, the hyperparameters used to train the model were optimised through empirical evaluation, by carefully observing the prediction performance using a set of candidate values of the hyperparameters; those included the number of neurons per layer, the number of hidden layers, dropout rates and the activation function used. The final design included bi-layered encoder and decoder, with the outmost layers having neurons in the order of $2 \times n_features$, where $n_features$ is the number of dynamic predictor variables used (14 for COVID-19 and 30 in the pneumonia and CKD studies). A dropout rate of 0.5 was used between each two layers to prevent the autoencoder from overfitting the training data and an adaptive learning rate was used using the Adam optimizer and starting at 0.001. The number of epochs was 1,000, which was selected via cycles of experiments and careful monitoring of the validation loss. An early stopping criteria was used to retain the best model by minimising the validation loss with a patience parameter of 50 epochs. All layers of the autoencoder used ReLU as their activation function, which performed best during our evaluation. The *Static-OP* module was implemented using the XGBoost algorithm. The parameters were chosen through a grid-search over the hyperparameter space. *Static-OP*'s sample weights were set to *Dynamic-KD*'s prediction errors.

D. Results

We evaluate *KD-OP*'s performance across four dimensions. First, we evaluate the performance under different settings presented by the three datasets; these include cohort heterogeneity with respect to individual characteristics and outcome distribution with respect to the minority (positive) cases. Here, we initially report metrics averaged across the different prediction intervals for each setting to obtain an overall view, and subsequently evaluate the model's robustness across different prediction intervals. We then evaluate the contributions of

the two modules *Dynamic-KD* and *Static-OP* to the overall performance, validating those empirically and against clinical knowledge. Finally, we compare the predictive power of *KD-OP* with existing outcome prediction models as reported in the literature. After evaluating *KD-OP*'s performance, we demonstrate its visualisation capability in section VI-D.5.

Throughout the experiments, we report the Precision-Recall Area Under the Curve (PR-AUC) to capture the model's performance with respect to the minority cases, as well as the widely-used Receiver-Operator Area Under the Curve (ROC-AUC). Despite our knowledge of ROC-AUC's impartial assessment of the model's performance under positive and negative outcomes [20], we choose to show it here due to its wide usage in the literature. Specifically, we use ROC-AUC to compare our model's performance with state-of-the-art models in section VI-D.4. We also report the macro-averaged precision, recall and F1-score. We used macro averages to understand the modules' true performance with respect to the under-represented outcomes [12].

1) *Overall Performance and Sample Diversity*: We first evaluate the overall performance across the three case studies. For each dataset, Table II shows the model's performance averaged across the prediction intervals of 5, 7, 14 and 30 days for each outcome. As the table shows, the performance is high overall. However, better performance across prediction intervals was obtained using the COVID-19 dataset compared pneumonia and CKD, despite the latter two being larger datasets with a higher resolution of observations (half-hourly intervals as opposed to two-hourly intervals used to construct the COVID-19 time-series). A close evaluation is shown in Figure 4, where higher performance ranges appear to be closely correlated with sample homogeneity (lower standard deviation) in age (shown in the legends) and the number of pre-existing conditions (reflected by the lightness of the plot circles).

COVID-19 admissions show a higher uniformity in age and pre-existing conditions, which consequently influences the patterns of changes in their physiological states. In both pneumonia and CKD, the diversity in the number of pre-existing conditions is starker (darker circles) in younger patients where lower-performance is achieved by the model.

2) Performance Across Prediction Intervals and Outcome Distribution Settings

Figure 5 shows *KD-OP*'s performance in predicting mortality and ICU admission/re-admission over 5, 7, 14 and 30-day intervals on COVID-19, pneumonia and CKD. Two observations can be made when examining this figure in conjunction with the distribution of the outcomes of Table I. Apart from 5-day ICU re-admission in pneumonia and CKD, (a) *KD-OP* shows high performance across short and long-term intervals, and (b) *KD-OP*'s performance remains high when the minority (positive) samples constitute $< 10\%$ of the overall population, which confirms the merit of relying on outlier detection to construct the temporal representation used in the pipeline. These findings are in-line with the demographic diversity results of Section VI-D.1, as the mean and standard deviations of age and number of pre-existing conditions of those re-admitted to the ICU within 5 days were

⁵The source is available at: <https://github.com/zibrahim/StackedPredictor/>

	COVID-19		Pneumonia		CKD	
	Mortality	ITU Admission	Mortality	ITU Readmission	Mortality	ITU Readmission
Avg Macro Prec	0.942 (0.895-0.966)	0.986 (0.972-0.996)	0.953(0.949-0.961)	0.889(0.737-0.981)	0.953 (0.922-0.981)	0.894 (0.760-0.985)
Avg Macro Rec	0.938 (0.907-0.969)	0.970 (0.963-0.984)	0.884(0.865-0.892)	0.869(0.825-0.926)	0.953 (0.853-0.906)	0.889 (0.802-0.985)
Avg Macro F1	0.936 (0.913-0.963)	0.977 (0.976-0.978)	0.901(0.90-0.984)	0.881(0.774-0.951)	0.912 (0.883-0.935)	0.919 (0.781-0.985)
Avg PR-AUC	0.969 (0.927-0.989)	0.987 (0.985-0.995)	0.905(0.880-0.993)	0.852(0.727-0.967)	0.916(0.869-0.958)	0.895 (0.756-0.998)
Avg ROC-AUC	0.931 (0.896-0.942)	0.971 (0.969-0.987)	0.884(0.865-0.892)	0.870(0.825-0.926)	0.878(0.853-0.908)	0.911 (0.826-0.985)

TABLE II: Average performance per outcome for COVID-19, pneumonia and CKD.

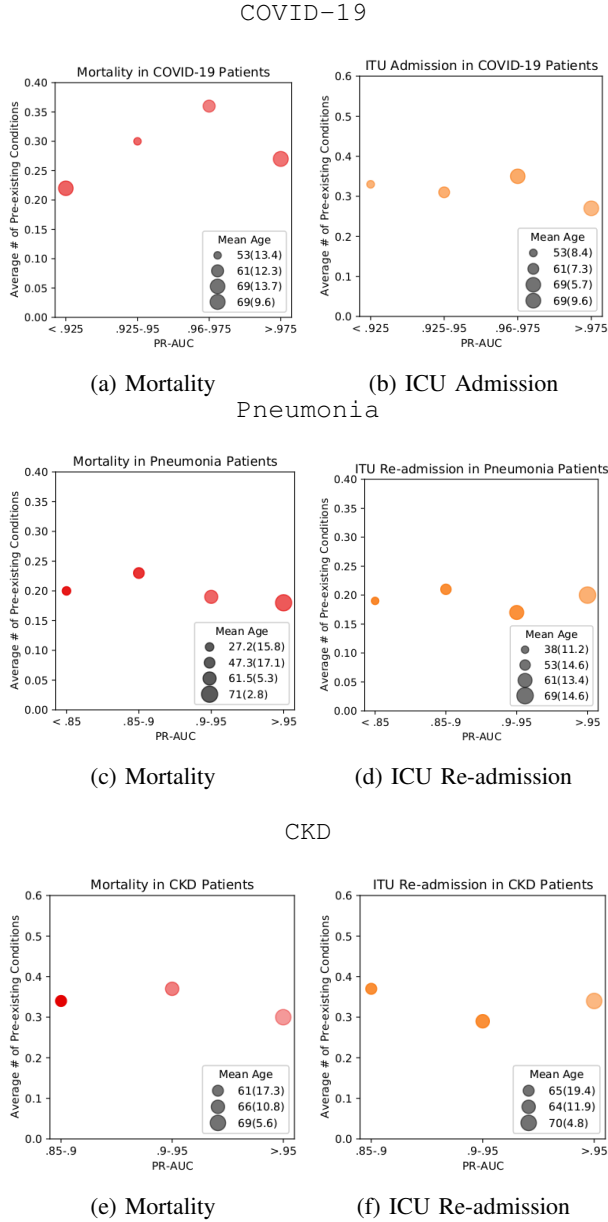


Fig. 4: Binned average performance for mortality (red) and ICU admission/re-admission (orange) measured in PR-AUC, highlighting the average and deviation in age and pre-existing conditions. Age mean and standard deviation are represented by circle size, while circle opacity represents the deviation of the number of pre-existing conditions from the mean.

33.76 (35.1) and 0.23 (0.2) for pneumonia and 66.12(21.3) and 0.28(0.17) for CKD respectively, showing a highly diverse sample almost deviating as highly as the overall pneumonia

and CKD populations as shown in table I. In contrast, the 5-day ICU admission sample in the COVID-19 study had a mean and standard deviation of age and number of pre-existing conditions being 63.3 (9.79) and 0.32 (0.05) respectively, showing a narrow range of demographical variation compared to pneumonia and CKD.

3) *The Contribution of Static-OP vs Dynamic-KD*: We now turn to compare the relative contribution of the two modules to *KD-OP*'s overall prediction across the three use cases, outcomes and four intervals. The detailed comparison is provided in table III. In the table, we list the contribution of each module per prediction interval for each outcome using macro-averaged precision, recall and F1 score, as well as PR-AUC and ROC-AUC. We also show **avg Δ** , the average change in each metric's value between *Dynamic-KD* and the final prediction made by *KD-OP*. It is clear that the two modules complement each other to reach a high performance that is not otherwise achievable by the time-series predictor alone. This effect is especially noticeable in recall, where *Static-OP* significantly increases **avg Δ** . In mortality outcomes, the stacked model slightly decreases the precision of *Dyanmic-KD*, but the magnitude of the decrease (**avg Δ**) is insignificant compared to the increase in recall.

Examining the performance from a domain angle, *Static-OP*'s contribution to the overall performance appears to be more pronounced in short-term outcomes. A highly noticeable difference is in the case of COVID-19 5-day mortality, where the average macro F1 score increases by 0.127 (from 0.786 using *Dynamic-KD* alone to 0.913 using the full pipeline). In contrast, the increase in F1 goes down to 0.021 (from 0.922 to 0.943) when examining 30-day mortality. This observation is consistent with current knowledge and recent findings that demographic information (e.g. age, pre-existing conditions) are highly predictive of short-term mortality in COVID-19 patients [56]. Similarly, for ICU readmission, replicated studies have found co-morbidities to be highly predictive of intensive care readmission during the same hospitalization [21].

4) Comparison with Existing Outcome Prediction Models:

Here, we compare *KD-OP*'s performance with the reported performance of relevant models and studies for outcome detection, showing the results in Table IV. Having gone through the literature, the only machine learning frameworks found to have been validated in nonICU settings are DEWS [49], eCART [7], and LightGBM [30] so we list those first. As the NEWS2 score is widely used to predict deterioration, we include the latest evaluation of its performance (from [22]) in the table for comparison. For these models, we compare their performance against the average performance of *KD-OP* when applied to the COVID-19 use-case, as it is a general ward

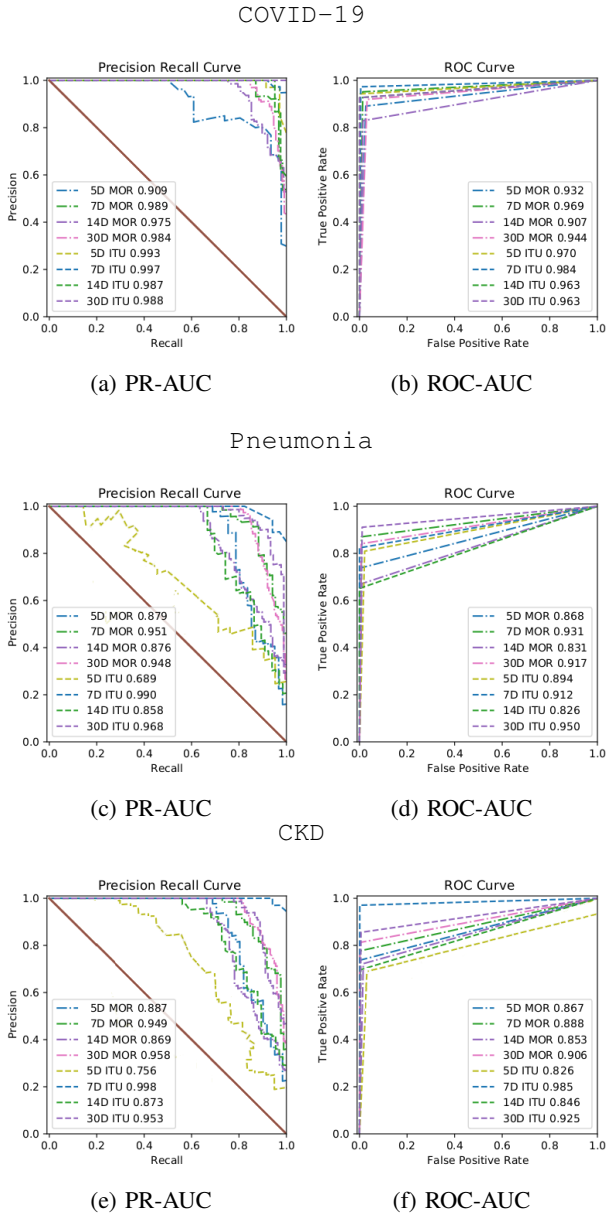


Fig. 5: Performance measured in PR-AUC (top) and ROC-AUC (bottom) for COVID-19, Pneumonia and CKD. In each plot, the respective performance is shown over 5, 7, 14 and 30 days for mortality and ICU admission (in the COVID-19 case) or ICU re-admission (in the pneumonia and CKD cases).

population. For each model, we highlight the class distribution of the target outcome as reported by each model's experimental evaluation settings. For *KD-OP*, the class distribution was taken as the average distribution of the outcomes over the intervals evaluated (5, 7, 14 and 30 days), as shown in Table I. As none of the models reports PR-AUC, we compiled a list of all reported metrics, using them to compare against *KD-OP*'s performance in conjunction with the widely-used ROC-AUC.

For mortality, LightGBM achieved a high ROC-AUC of 0.961 with a class distribution of 5.1% of the outcome. However, the only other available metric for LightGBM is specificity, which is at a low 0.641 and entails a high rate

Dataset	Outcome	Model	Average Macro Pr	Average Macro Rec	Average Macro F1	PR-AUC	ROC-AUC
General (COVID)	5MOR	Dyn-KD	0.967	0.717	0.786	0.553	0.683
		KD-OP	0.895	0.932	0.913	0.909	0.932
		Dyn-KD	0.981	0.882	0.927	0.855	0.887
		KD-OP	0.972	0.984	0.978	0.989	0.969
	14MOR	Dyn-KD	0.958	0.824	0.871	0.782	0.823
		KD-OP	0.946	0.907	0.925	0.975	0.907
	30MOR	Dyn-KD	0.965	0.893	0.922	0.885	0.895
		KD-OP	0.941	0.944	0.943	0.984	0.944
	Avg Δ		-0.029	+0.128	+0.065	+0.257	+0.119
	5ICU	Dyn-KD	0.958	0.897	0.925	0.853	0.932
		KD-OP	0.983	0.970	0.976	0.993	0.970
	7ICU	Dyn-KD	0.994	0.932	0.961	0.885	0.887
		KD-OP	0.983	0.970	0.976	0.997	0.984
ICU (Pneum)	14ICU	Dyn-KD	0.979	0.826	0.950	0.782	0.823
		KD-OP	0.996	0.963	0.979	0.987	0.963
	30ICU	Dyn-KD	0.983	0.962	0.972	0.994	0.999
		KD-OP	0.996	0.963	0.979	0.988	0.963
	Avg Δ		+0.007	+0.245	+0.026	+0.107	+0.059
	5MOR	Dyn-KD	0.988	0.736	0.896	0.72	0.8
		KD-OP	0.954	0.891	0.919	0.879	0.868
	7MOR	Dyn-KD	0.984	0.841	0.997	0.765	0.862
		KD-OP	0.961	0.892	0.923	0.951	0.931
	14MOR	Dyn-KD	0.984	0.841	0.897	0.73	0.802
		KD-OP	0.949	0.865	0.90	0.876	0.831
	30MOR	Dyn-KD	0.972	0.878	0.916	0.861	0.885
		KD-OP	0.967	0.888	0.921	0.948	0.894
	Avg Δ		-0.024	+0.035	-0.011	+0.047	+0.044
ICU (CKD)	5ICU	Dyn-KD	0.648	0.684	0.679	0.587	0.643
		KD-OP	0.737	0.825	0.774	0.689	0.894
	7ICU	Dyn-KD	0.994	0.853	0.999	0.967	0.926
		KD-OP	0.981	0.926	0.951	0.990	0.912
	14ICU	Dyn-KD	0.980	0.742	0.816	0.561	0.713
		KD-OP	0.904	0.835	0.866	0.858	0.826
	30ICU	Dyn-KD	0.856	0.818	0.899	0.764	0.828
		KD-OP	0.981	0.894	0.932	0.968	0.950
	Avg Δ		+0.031	+0.096	+0.032	+0.123	+0.086
	5MOR	Dyn-KD	0.988	0.836	0.896	0.766	0.799
		KD-OP	0.959	0.897	0.915	0.887	0.867
	7MOR	Dyn-KD	0.984	0.841	0.915	0.728	0.855
		KD-OP	0.981	0.901	0.947	0.949	0.888
	14MOR	Dyn-KD	0.967	0.807	0.863	0.728	0.806
		KD-OP	0.959	0.863	0.902	0.869	0.853
	30MOR	Dyn-KD	0.968	0.879	0.916	0.862	0.903
		KD-OP	0.974	0.906	0.935	0.958	0.906
	Avg Δ		-0.009	+0.050	+0.027	+0.145	+0.0375
	5ICU	Dyn-KD	0.612	0.646	0.665	0.658	0.733
		KD-OP	0.727	0.772	0.739	0.756	0.826
	7ICU	Dyn-KD	0.994	0.853	0.911	0.778	0.890
		KD-OP	0.985	0.985	0.985	0.998	0.985
	14ICU	Dyn-KD	0.908	0.743	0.816	0.705	0.714
		KD-OP	0.948	0.846	0.920	0.873	0.846
	30ICU	Dyn-KD	0.984	0.861	0.941	0.785	0.859
		KD-OP	0.962	0.925	0.942	0.953	0.925
	Avg Δ		+0.016	+0.106	+0.064	+0.163	+0.095

TABLE III: Detailed comparison of the performance of Dynamic-KD with the final prediction made by KD-OP across all three case studies. The comparison is detailed by prediction interval (5, 7, 14 and 30 days) and by outcome (mortality, ICU admission/re-admission).

of false alarms generated by the framework. eCart's ROC-AUC is equally distinctive at 0.93 with extremely low frequencies of mortality cases in the data used (1.2 % of the cases). However, no information on the recall or specificity of the model is available. We, therefore, draw attention the only outcome for which eCart's sensitivity and specificity are investigated, which is cardiac arrest. For this outcome, despite the high ROC-AUC achieved by the model (0.89) at a very low distribution rate of the outcome variable (0.05%), specificity is at 0.52%, which once again shows the over-optimism of the ROC-AUC reported by the model. *KD-OP* achieved a ROC-AUC of 0.978, with mortality averaging at 18.1% of the samples (ranging between 10.88-26.23%). DEWS' AUC score was also high at 0.926. However, the class distribution reported in their study is highly skewed in favour of the outcome (65.3% mortality). With respect to unplanned ICU admissions, *KD-OP* achieved the highest AUC

Model	Primary Outcome	Outcome Distribution	AUC	PR-AUC	Sensitivity	Specificity
General Ward						
NEWS2 [22]	Deterioration (1 day)	(94.8%, 5.2%)	0.78 (0.73 - 0.83)	NA	0.28 (0.21 - 0.37)	0.80 (0.79 - 0.82)
eCART [7]	Unplanned ICU Admission,	(95%, 5%)	0.75 (0.74-0.75)	NA	NA	NA
	Mortality	(98.8%, 1.2%)	0.93 (0.93-0.93)	NA	NA	NA
	Cardiac Arrest	(99.5%, 0.05%)	0.89 (0.88-0.91)		0.89 (0.88-0.91)	0.52 (0.52-0.52)
DEWS [49]	Unplanned ICU Admission	(72.8%, 27.2%)	0.811 (0.811 - 0.822)	NA	0.555 (0.554 - 0.557)	0.90 (0.90 - 0.90)
	Mortality	(35.7%, 65.3%)	0.926 (0.926 - 0.927)	NA	0.831 (0.831 - 0.832)	0.888 (0.888 - 0.888)
LightGBM [30]	Mortality	(94.9%, 5.1%)	0.961 (NA)	NA	NA	0.641
KD-OP (General Ward)	Mortality	(82.9%, 18.1%)	0.927 (0.9 - 0.932)	0.964 (0.941 - 0.969)	0.905 (0.89 - 0.91)	0.94 (0.935 - 0.945)
	Unplanned ICU Admission	(91.19%, 8.81%)	0.981 (0.98 - 0.984)	0.992 (0.992 - 0.992)	0.99 (0.99-0.99)	0.99 (0.99 -0.99)
ICU Settings						
SANMF [35]	Mortality	(89.98%, 10.02%)	0.848 (0.846, 8.84)			
SICULA [42]	Mortality	(88.76%, 12.24%)	0.88 (0.87-0.89)	NA	NA	NA
KD-OP (ICU)	Mortality	(89.05%, 10.95%)	0.881 (0.880 - 0.885)	0.911 (0.910 - 0.913)	0.953 (0.903 - 0.969)	0.918 (0.88 - 0.931)
COVID-19						
Carr [6]	Deterioration (14 days)	-	0.78 (0.74 - 0.82)			
Guo [18]	Deterioration (14 days)	-	0.67 (0.61 - 0.73)			
Liu [24]	Mortality & Deterioration	-	0.74 (0.69 - 0.79)			
Galloway [14]	Deterioration	-	0.72 (0.68 - 0.77)			
Gong [16]	Deterioration	-	0.853 (0.790- 0.916)			

TABLE IV: Comparison of KD-OP's performance with existing literature of general outcome prediction tested in general wards and ICU settings. Additionally, a comparison with current statistical models of to predict deterioration in COVID-19 is given.

of 0.981 with an average class distribution of 8.81% (ranging between 8.22 -9.71%) for the four intervals. DEWS was the closest competitor at 0.811 AUC, albeit with a significantly higher distribution of the positive outcome (27%). Overall, *KD-OP* shows the highest performance stability across the two outcomes, rendering it a better candidate for general hospitalisation outcome prediction; especially given the lack of thorough assessment of competitive models using metrics suitable for the problem under study.

We also list high-performing machine learning models that have only been strictly validated in ICU settings; those include SANMF [35], SICULA (a.k.a. the super learner) [42] and [38]. It is worth noting that none of the models predicts ICU re-admission. We, therefore, resort to comparing with *KD-OP*'s average performance in predicting mortality when applied to pneumonia and CKD using the MIMIC-III ICU dataset. Also, apart from [38], which reports sensitivity, the models strictly rely on ROC-AUC in reporting their performance. We will, therefore resort to comparing with *KD-OP*'s performance using ROC-AUC. As the table shows, *KD-OP* is the best predictor of mortality in an ICU setting, marginally exceeding SICULA's performance (ROC-AUC of 0.881 vs 0.880). Given that the SICULA's performance is the current benchmark for mortality prediction in the ICU, *KD-OP*'s performance is well-aligned with existing prediction potential.

Finally, as the literature now contains several statistical models aiming to make prognostic predictions of COVID-19 hospital admissions, we compare those with *KD-OP* applied to the COVID-19 case. It is worth noting that all of the listed under the COVID-19 section of table IV are scoring systems aiming to mimic or exceed the performance of NEWS2 in predicting COVID-19 deterioration. Hence, *KD-OP* presents a novel contribution to the COVID-19 use case in being a scalable end-to-end machine learning architecture for predicting hospitalisation outcomes for COVID-19 admissionS.

5) Visual Justification of Predicted Outcomes: The stacked nature of *KD-OP* naturally enables visualising its predictions using the built-in visualisation properties of each module and obtaining the relative contributions of each module's predic-

tion to the outcome. For *Dynamic-KD*, the feature attention weights at each time interval make up the relative importance of the temporal signatures of each feature. On the other hand, the gradient boost implementation of *Static-OP* provides a feature importance capability, which we use to understand the relative contribution of each static feature. Since the relative contribution of each module to the final prediction is outcome and interval dependent, including it in the visualisation of the output is highly essential for clinical utility as it directs the attention to the most contributing view (static or dynamic) of the patient. We define the contribution of each module using the ratios of the respective modules' PR-AUC.

An example of the generated visualisation of a positive 30-day mortality outcome of a COVID-19 patient is shown in figure 6. In the figure, the left-most bar shows the relative contribution of the individual modules. In this scenario, *Dynamic-KD* is a significant contributor ($\approx 93\%$ of the overall contribution). Examining the attention weights generated by the framework shows that the highest weights are of lymphocytes and neutrophils (Lymph and Neut in the figure) at hours 36-48 as well as C-reactive protein (CRP in the figure) at time-step 48 (24th hour). We use this information as a justification for the prediction made by *Dynamic-KD*. On the other hand, the patient's age and the mean NEWS2 score show the highest importance among the static features, followed by the length of the period from symptoms to admission (SxToAdmit) and the maximum C-reactive protein level over the 24 hours.

It is essential to view this justification in relation to current findings. C-reactive protein, lymphocytes and lactic dehydrogenase have been recently found to be highly correlated with adverse outcomes in COVID-19 patients [57]. Although lactic dehydrogenase was not part of our COVID-19 dataset, the temporal signatures of both C-reactive protein and lymphocytes have been accurately identified by *Dynamic-KD* as predictors of the particular patient's outcome. This, in addition to age being marked as an important static feature, agrees with recent findings [56], showing that the signals jointly picked up by the framework's modules are coherent and well-aligned with clinical findings.

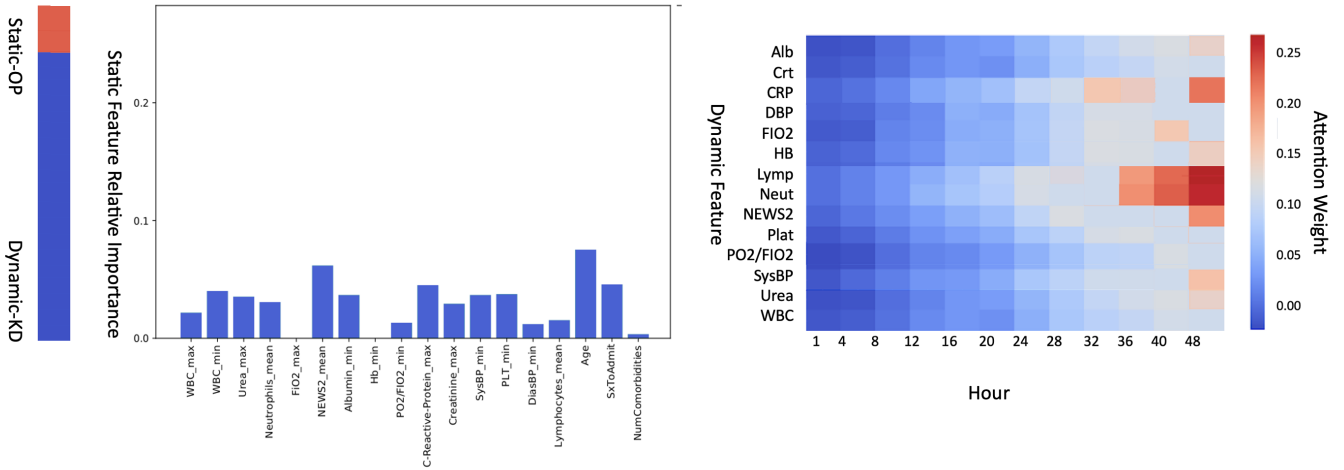


Fig. 6: Visual Justification of KD-OP's Predictions

VII. DISCUSSION

We developed and validated *KD-OP*, an end-to-end pipeline for predicting adversity during hospitalisation. The pipeline comprises two stacked modules, each making predictions from a view of the patient's data: dynamic time-series and static features. The stacking of the pipeline's modules enables mimicking a clinician's approach to making prognostic decisions, by taking into account the interplay between the temporal signatures of a patient's physiology as well as time-invariant characteristics. By design, the pipeline is cognizant of the class imbalance natural to hospitalisation outcome data. It is trained and validated using stratified data that retains the original distribution of the real outcomes within the population. The pipeline's visualisation component complements its prediction by providing visual interpretations to aid clinical decision making. The visual interpretation provided by *KD-OP* is unique in that it accounts for the interplay between dynamic and static features in justifying the predictions made by the pipeline; a feature that derives directly from the stacked architecture. To our knowledge, this feature is not available in any existing hospitalisation outcome predictor.

We evaluated *KD-OP*'s performance using real hospital data on three use cases representative of the diversity of electronic health records data. Using the pipeline to predict mortality and ICU admission/re-admission over 5-day, 7-day, 14-day, and 30-day intervals resulted in prediction accuracies exceeding 90% in all mortality outcomes and most of the ICU admission/re-admission outcomes.

A disease-agnostic model such as *KD-OP* could be built into the visual display of an EHR for all clinicians to use. The challenge at the moment is that each hospital department has its outcome prediction scoring system, subsequently making it unrealistic to build over 30 distinct models into an EHR system. The generic nature of *KD-OP*, coupled with high performance and visualisation capability, gives it a broader potential for integration in ICU and nonICU settings.

There are several possible avenues to build on the existing framework. First, it would be interesting to design a modified

platform which projects the progression of the risk of adversity; we are currently developing a temporal risk score model to predict and visualise the risk of a given outcome on an individual level over time, using *KD-OP* as the base model. Second, the pipeline currently only supports classification outcomes, which limits its utility. Existing targets include the prognosis of continuous outcomes such as worsening oxygenation and worsening of cardiac function. Also, the current framework strictly uses routinely collected clinical variables as predictors. Other types of data can be of high relevance to a given use case. For example, ECG signals are the predictors of choice for cardiology-related outcomes; X-ray images can positively improve predictive power in the case of COVID-19, etc. Although the stacked architecture has proven to be highly robust compared to parallel ensembles, it is intrinsically less flexible towards extensions to incorporate additional models. It is, therefore, an interesting research problem to address, exploring the avenues of further extending the stacked model.

Our final word pertains to all outcome prediction models. The development of a useful clinical tool requires full engagement with stakeholders and ongoing clinical assessment of its validity. Numerous scoring systems have been developed over the decades, but few are routinely used because many are developed in isolation of the clinical teams. Therefore, strengthening academic and clinical collaboration is key to the success of any model.

REFERENCES

- [1] M Aczon, D Ledbetter, L Ho, and et al. Dynamic mortality risk predictions in pediatric critical care using recurrent neural networks. *ArXiv*, abs/1701.06675, 2017.
- [2] Intensive Care National Audit and Research Centre. Key statistics from the case mix programme april 2011-march 2012. *Intensive Care National Audit and Research Centre*, 2013.
- [3] A Awad, M Bader-El-Den, J McNicholas, and et al. Early hospital mortality prediction of intensive care unit patients using an ensemble learning approach. *International Journal of Medical Informatics*, 108:185–195, 10 2017.
- [4] N Brajer, B Cozzi, M Gao, and et al. Prospective and External Evaluation of a Machine Learning Model to Predict In-Hospital Mortality of Adults at Time of Admission. *JAMA Network Open*, 3(2):e1920733–e1920733, 2020.

- [5] P Branco, L Torgo, and R Ribeiro. A survey of predictive modeling on imbalanced domains. *ACM Computing Surveys*, 49(2), 2016.
- [6] E Carr, R Bendayan, D Bean, and et al. Evaluation and improvement of the national early warning score (news2) for covid-19: a multi-hospital study. 2020.
- [7] MM Churpek, TC Yuen, C Winslow, and et al. Multicenter development and validation of a risk stratification tool for ward patients. *American Journal of Respiratory Critical Care Medicine*, 190(6):649–55, 2014.
- [8] R Das and D Wales. Machine learning landscapes and predictions for patient outcomes. *Royal Society open science*, 4(7):170175, 2017.
- [9] J Davis and M Goadrich. The relationship between precision-recall and roc curves. In *Machine Learning*, pages 233–240, 2006.
- [10] S Dzeroski and B Zenko. Is combining classifiers with stacking better than selecting the best one? *Machine Learning*, 54:255–273, 2004.
- [11] C Feng, H Wang, N Lu, and et al. Log-transformation and its implications for data analysis. *Shanghai Arch Psychiatry*, 26(2):105–109, 2014.
- [12] H Fernandez, L Garcia, P Galar, and et al. *Learning from Imbalanced Data Sets*, page 25. Springer, 1 edition, 2018.
- [13] C Ferri, J Hernandez-Orallo, and R Modroiu. An experimental comparison of performance measures for classification. *Pattern Recognition Letters*, 30(1):27 – 38, 2009.
- [14] J Galloway, S Norton, R Barker, and et al. A clinical risk score to identify patients with covid-19 at high risk of critical care admission or death: An observational cohort study. *Journal of Infection*, 81, 05 2020.
- [15] Z Ghrib, R Jaziri, and R Romdhane. Hybrid approach for anomaly detection in time series data. In *International Joint Conference on Neural Networks (IJCNN)*, pages 1–7, 2020.
- [16] J Gong, H Dong, S Xia, and et al. Correlation analysis between disease severity and inflammation-related parameters in patients with covid-19 pneumonia. 2020.
- [17] P Griffiths, A Maruotti, S Recio, and et al. Nurse staffing, nursing assistants and hospital mortality: retrospective longitudinal cohort study. *BMJ Quality and Safety*, 28(8):609–617, 2019.
- [18] T Guo, Y Fan, M Chen, and et al. Cardiovascular Implications of Fatal Outcomes of Patients With Coronavirus Disease 2019 (COVID-19). *JAMA Cardiology*, 5(7):811–818, 07 2020.
- [19] T Guo, T Lin, and N Antulov-Fantulin. Exploring interpretable LSTM neural networks over multi-variable data. In *Machine Learning Research*, pages 2494–2504, 2019.
- [20] H Haibo and M Yunqian. *Imbalanced Learning: Foundations, Algorithms, and Applications*, page 27. Wiley-IEEE Press, 1 edition, 2013.
- [21] K Ho, G Dobb, K Lee, and et al. The effect of comorbidities on risk of intensive care readmission during the same hospitalization: a linked data cohort study. *Journal of Critical Care*, 24(1):101–107, 2009.
- [22] L Hodgson, J Congleton, R Venn, and et al. NEWS 2 - too little evidence to implement? *Clinical medicine*, 18(5):371–373, 2018.
- [23] MS Islam, TN Poly, B Walther, and et al. Prediction of sepsis patients using machine learning approach: A meta-analysis. *Computer methods and programs in biomedicine*, 170:1–9, 2019.
- [24] Liu J, Zhang S, Wu Z, and et al. Clinical outcomes of covid-19 in wuhan, china: a large cohort study. *Annals of Intensive Care*, 10:282–288, 12 2020.
- [25] A Johnson, T Pollard, L Shen, and et al. MIMIC-III, a freely accessible critical care database. *Scientific Data*, 3(1):160035, 2016.
- [26] J Johnson, O Bjornsson, P Andersson, and et al. Artificial neural networks improve early outcome prediction and risk classification in out-of-hospital cardiac arrest patients admitted to intensive care. *Critical Care*, 24(1):474, 2020.
- [27] G Ke, Q Meng, T Finley, and et al. LightGBM: a highly efficient gradient boosting decision tree. *Advances in Neural Information Processing Systems*, 30:3146–3154, 2017.
- [28] T Kieu, B Yang, C Guo, and C Jensen. Outlier detection for time series with recurrent autoencoder ensembles. In *Proceedings of the Twenty-Eighth International Joint Conference on Artificial Intelligence, IJCAI-19*, pages 2725–2732. International Joint Conferences on Artificial Intelligence Organization, 7 2019.
- [29] T Kieu, B Yang, and CS Jensen. Outlier detection for multidimensional time series using deep neural networks. In *IEEE MDM*, pages 125–134, 2018.
- [30] J Kobylarz, H Dos-Santos, F Barletta, and et al. A machine learning early warning system: Multicenter validation in brazilian hospitals. In *IEEE CBMS*, pages 321–326, 06 2020.
- [31] WC Lee, YT Lee, LC Li, and et al. The number of comorbidities predicts renal outcomes in patients with stage 3-5 chronic kidney disease. *Journal of Clinical Medicine*, 7(12):493, 2018.
- [32] A Leontjeva and I Kuzovkin. Combining static and dynamic features for multivariate sequence classification. In *IEEE DSAA*, pages 21–30, 10 2016.
- [33] X Li, D Zhu, and P Levy. Predicting clinical outcomes with patient stratification via deep mixture neural networks. In *AMIA*, pages 367–376, 2020.
- [34] V Liu, Y Lu, K Carey, and et al. Comparison of early warning scoring systems for hospitalized patients with and without infection at risk for in-hospital mortality and transfer to the intensive care unit. *JAMA Network Open*, 3(5):e205191, 2020.
- [35] Y Luo, X Yu, R Joshi, and et al. Predicting icu mortality risk by grouping temporal trends from a multivariate panel of physiologic measurements. In *AAAI Conference on Artificial Intelligence*, pages 42–50, 2016.
- [36] P Malhotra, A Ramakrishnan, G Anand, and et al. Lstm-based encoder-decoder for multi-sensor anomaly detection. *CoRR*, abs/1607.00148, 2016.
- [37] M Mallappallil, EA Friedman, BG Delano, and et al. Chronic kidney disease in the elderly: evaluation and management. *Clinical Practice*, 11(5), 2014.
- [38] M Moreno-García, J González-Robledo, F Martín-González, and et al. Machine learning methods for mortality prediction of polytraumatized patients in intensive care units – dealing with imbalanced and high-dimensional data. In *Intelligent Data Engineering and Automated Learning*, pages 309–317, 2014.
- [39] E Muthumbi, BS Lowe, C Muyodi, and et al. Risk factors for community-acquired pneumonia among adults in kenya: a case-control study. *Pneumonia*, 9:17, 2017.
- [40] J Nogos, S Khan, and A Mihailidis. Fall detection from thermal camera using convolutional lstm autoencoder. EasyChair Preprint no. 824, EasyChair, 2019.
- [41] F Perrotta, G Corbi, G Mazzeo, and et al. COVID-19 and the elderly: insights into pathogenesis and clinical decision-making. *Aging Clinical and Experimental Research*, 32(8):1599–1608, 2020.
- [42] R Pirracchio. Mortality prediction in the ICU based on MIMIC-II results from the Super ICU Learner Algorithm (SICULA) project, pages 295–313. 09 2016.
- [43] R Raj, T Luostarinen, E Pursiainen, and et al. Machine learning-based dynamic mortality prediction after traumatic brain injury. *Nature Scientific Reports*, 9:17672, 2019.
- [44] Royal College of Physicians. National Early Warning Score (NEWS) 2: Standardising the assessment of acute-illness severity in the NHS. 2017.
- [45] U Schmidt-Erfurth, A Sadeghipour, B Gerendas, and et al. Artificial intelligence in retina. *Progress in Retinal and Eye Research*, 67:1–29, 2018.
- [46] P Schwab, GC Scebbba, J Zhang, and et al. Beat by beat: Classifying cardiac arrhythmias with recurrent neural networks. In *2017 Computing in Cardiology (CinC)*, pages 1–4, 2017.
- [47] F Shamout, Y Shen, N Wu, and et al. An artificial intelligence system for predicting the deterioration of covid-19 patients in the emergency department. *ArXiv*, 08 2020.
- [48] F Shamout, T Zhu, and D Clifton. Machine learning for clinical outcome prediction. *IEEE Reviews on Biomedical Engineering*, 2020.
- [49] F Shamout, T Zhu, P Sharma, and et al. Deep interpretable early warning system for the detection of clinical deterioration. *IEEE Journal of Biomedical and Health Informatics*, PP:1–1, 09 2019.
- [50] S Shashikumar, A Shah, G Clifford, and et al. Detection of paroxysmal atrial fibrillation using attention-based bidirectional recurrent neural networks. In *ACM SIGKDD*, pages 715–723, 2018.
- [51] V Snorovichina and A Zaytsev. Unsupervised anomaly detection for discrete sequence healthcare data, 2020.
- [52] AD Storms, J Chen, LA Jackson, and et al. Rates and risk factors associated with hospitalization for pneumonia with icu admission among adults. *BMC Pulmonary Medicine*, 17:208, 2017.
- [53] H Thorsen-Meyer, AB Nielsen, AP Nielson, and et al. Dynamic and explainable machine learning prediction of mortality in patients in the intensive care unit: a retrospective study of high-frequency data in electronic patient records. *Lancet Digital Health*, 2(4):E179–91, 2020.
- [54] L Turgeman and J May. A mixed-ensemble model for hospital readmission. *Artificial Intelligence in Medicine*, 72:72?82, 08 2016.
- [55] X Xie, C Wang, S Chen, and et al. Real-time illegal parking detection system based on deep learning. In *ACM Deep Learning Technologies*, page 23–27, 2017.
- [56] A Yadaw, Y Li, S Bose, and et al. Clinical features of covid-19 mortality: development and validation of a clinical prediction model. *The Lancet Digital Health*, 2(10):E516–E525, 2020.

- [57] L. Yan, H. Zhang, and Y. Yuan. An interpretable mortality prediction model for covid-19 patients. *Nature Machine Intelligence*, 2:283–288, 2020.